Answers in Depth, Vol. 5 (2010)
www.answersingenesis.org/doc/articles/aid/v5/radioisotopes_diabase_bass_rapids.pdf

Radioisotopes in the Diabase Sill (Upper Precambrian) at Bass Rapids, Grand Canyon, Arizona: An Application and Test of the Isochron Dating Method

Andrew A. Snelling,, Ph.D., Answers in Genesis
Steven A. Austin, Ph.D., Institute for Creation Research
William A. Hoesch, Institute for Creation Research

This paper was originally published in the *Proceedings of the Fifth International Conference on Creationism*, pp. 269–284 (2003) and is reproduced here with the permission of the Creation Science Fellowship of Pittsburgh (www.csfpittsburgh.org).

Abstract

The five-point Rb-Sr whole-rock isochron age of 1.07 Ga for the diabase sill at Bass Rapids, Grand Canyon, has been regarded for 20 years as an excellent example of the application of conventional radioisotopic dating. Initial thorough isotopic mixing within the sill is ideal for yielding concordant whole-rock isochron and mineral isochron ages. However, our new K-Ar, Rb-Sr, Sm-Nd, and Pb-Pb radioisotope data from 11 whole-rock samples (eight diabase, three granophyre) and six mineral phases separated from one of the whole-rock diabase samples yield discordant whole-rock and mineral isochron 'ages.' These isochron 'ages' range from 841.5±164 Ma (whole-rock K-Ar) to 1375±170 Ma (mineral Sm-Nd). Although significant discordance exists between the K-Ar, Rb-Sr, Sm-Nd, and Pb-Pb radioisotope methods, each method appears to yield concordant 'ages' internally between whole rocks and minerals. Internal concordance is best illustrated by the Rb-Sr whole rock and mineral isochron 'ages' of 1055±46 Ma and 1059±48 Ma, respectively. It is therefore argued that only changing radioisotope decay rates in the past could account for these discordant isochron 'ages' for the same geologic event. Furthermore, these data are consistent with alpha decay having been accelerated more than beta decay, and with the longer the present half-life the greater being the acceleration factor.

Keywords

diabase, sill, Grand Canyon, potassium-argon, rubidium-strontium, samarium-neodymium, lead-lead, radioisotopic dating, model ages, whole-rock isochron ages, mineral isochron ages, discordance, decay constants, accelerated decay

Introduction

The 1.1-billion-year rubidium-strontium isochron date for the Cardenas Basalt is widely regarded as perhaps the best 'age' obtained for Grand Canyon strata.[1, 2] Similarly, the diabase sill at Bass Rapids (fig. 1) has yielded a 1.07-billion-year rubidium-strontium isochron date,[3] providing apparent confirmation of the relationship between the diabase sills and the Cardenas Basalt flows. The Bass Rapids diabase sill provides every indication that it was well mixed isotopically when it was intruded, even though during cooling the sill segregated mineralogically and chemically by crystal settling to produce a granophyre on top of the diabase. Such a condition of initial thorough isotopic mixing of the original magma body followed by rapid chemical segregation is suited to the assumptions of whole-rock and mineral isochron dating. How then are the radioisotope daughters distributed through the granophyre and diabase, and through the mineral phases of the latter? The various radioisotope pairs would be expected to give concordant whole-rock isochron and mineral isochron 'ages.' However, published potassium-argon model 'ages' for the diabase sills (and the Cardenas Basalt) are significantly younger than their associated rubidium-strontium isochron 'ages'.[4, 5]

Geologic Setting

Mafic igneous rocks occur as sills, dikes, and flows in the thick succession of strata making up the middle Proterozoic Unkar Group of the Grand Canyon, Arizona (fig. 1). The Unkar Group sedimentary sequence is comprised of four formations—in ascending order, the Bass Limestone, Hakatai Shale, Shinumo Quartzite, and the Dox Sandstone—which are overlain by the 300 meter plus thick flow sequence of lava flows of the Cardenas Basalt.[6, 7] The younger Precambrian sediments of the Nankoweap Formation and the Chuar Group overlie this Unkar Group succession, which unconformably rests on the early Proterozoic metamorphic and igneous crystalline basement.[8–10]

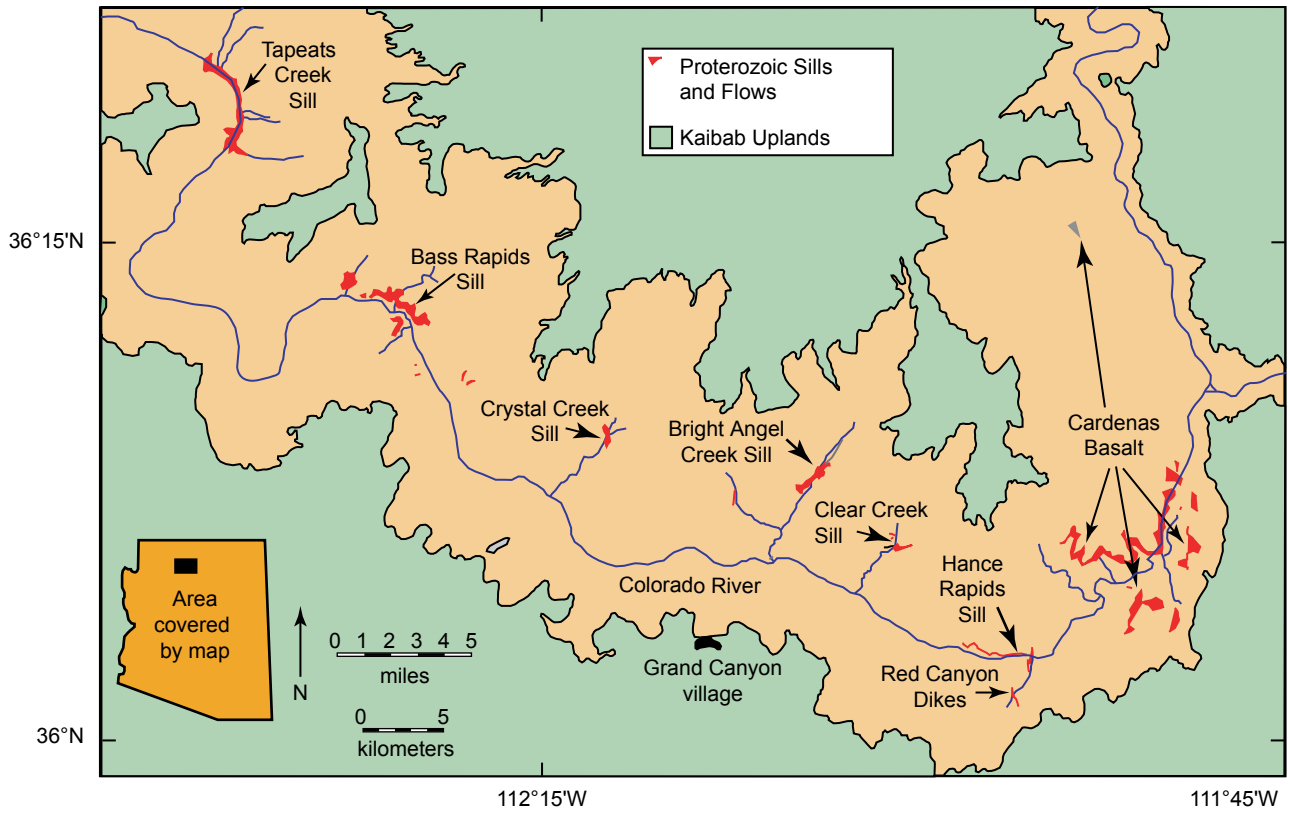

Fig. 1. Location of the Bass Rapids diabase sill in Grand Canyon, northern Arizona.

The diabase sills and dikes are believed to be the intrusive equivalents of the Cardenas lava flows, but they are not found in direct association with the Cardenas Basalt.[11–13] Thus the relationship between them is obscure because the direct feeders to the flows have never been recognized among the available diabase outcrops. The diabase sills are, in fact, confined to the lower part of the Unkar Group, particularly intruding near the boundary between the Bass Limestone and Hakatai Shale, while the related dikes are intruded into all the formations above the sills along faults that predate, or are contemporaneous with, the sills. These mafic sills crop out in seven locations along a 70–80 km length of the Grand Canyon (fig. 1), whereas the Cardenas Basalt flows are restricted to the area around Basalt Canyon in the eastern Grand Canyon. The sills range in thickness from 20 meters (about 65 feet) near Hance Rapids in the east to more than 200 meters (655 feet) near Tapeats Creek in the west. They are composed chiefly of medium-grained ophitic olivine-rich diabase that is uniform in texture and mineralogy from sill to sill in the Canyon. The dikes have a similar composition but are finer grained, as are the chilled margins of the sills. Early in-place differentiation and crystal settling in the sills is evidenced by granophyre layers up to 10 meters thick and felsite dikes, and by layers which are richer in olivine.

The thick sill near Bass Rapids was chosen for this study because not only are there good outcrop exposures of it, but because there is a well-defined 6 meter thick granophyre layer on top of the 85 meter thick diabase. Furthermore, more geochemical and radioisotopic analyses have been undertaken previously on this sill than any of the other sills.

Previous Work

Noble was the first to describe the diabase sills in the Bass Canyon-Shinumo Creek area.[14,15] Maxson[16,17] mapped the intrusive rocks of the Grand Canyon but did not describe the diabase sills and dikes. Detailed mapping and sampling of the sills and dikes, and the Cardenas Basalt flows, followed by petrographic examination and chemical analysis of the samples collected, were reported by Hendricks[18,19] and Hendricks and Lucchitta.[20] They found that chemical variation diagrams indicated a potential common parentage for the diabase in the sills and the lower third of the basalt flows. However, the flows in the upper two-thirds of the Cardenas Basalt sequence were found to be much more silicic than the diabase sills, and, therefore, it was concluded that they probably were not emplaced during the same phase of igneous activity. Nevertheless, the mineral composition of the unaltered basalt flows in the bottom third of the sequence is similar to that of the diabase sills, which suggested that those lavas and the diabase sills were co-magmatic and probably coeval. Thus, they concluded that the

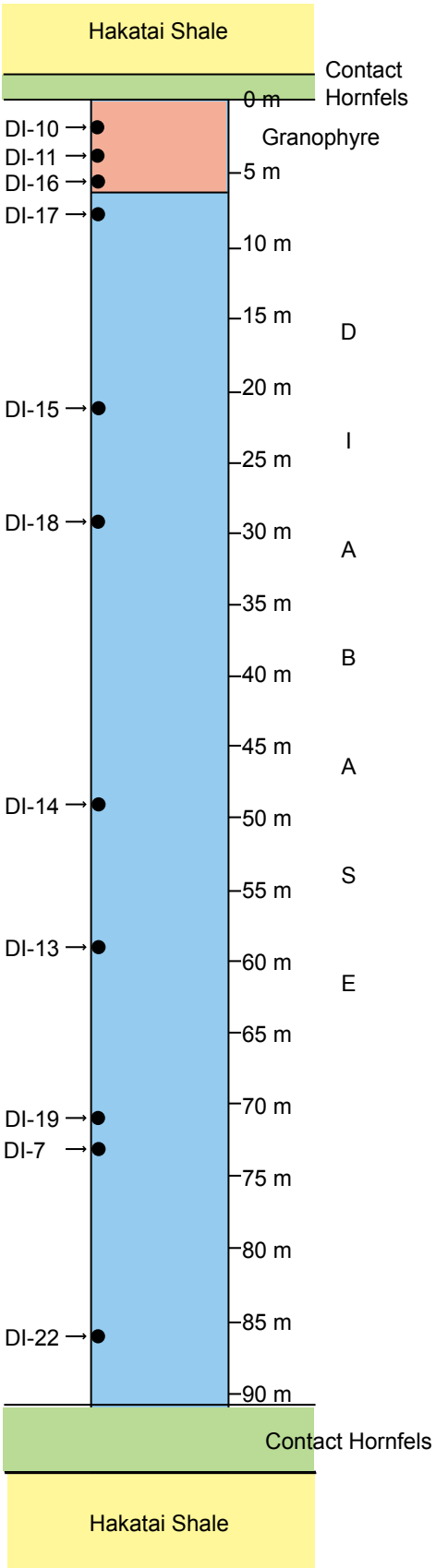

Fig. 2. Diagrammatic section through the Bass Rapids sill showing the granophyre 'capping' on the diabase, the contact hornfels, and the location of samples.

basalt lavas in the top two-thirds of the sequence were extruded after differentiation of the parent magma.

Paleomagnetic observations and radioisotopic age determinations by Elston and Grommé,[21] Elston and McKee,[22] and Elston[23] suggest that the diabase sills may be slightly older than the Cardenas Basalt flows, perhaps as much as 40–50 Ma. The isotopic (Rb-Sr) determinations yielded an age of 1090±70 Ma for the flows of the Cardenas Basalt,[24, 25] whereas the sill in the Shinumo Creek-Bass Canyon area had a five-point isochron age of 1070±30 Ma.[26] Although these ages are obviously identical, the flows and sills were found to have different initial $^{87}Sr/^{86}Sr$ ratios (0.70650±0.0015 and 0.70420±0.0007 respectively) and apparently distinctly different paleomagnetic pole positions. A K-Ar model age of 944 Ma was obtained on pyroxene extracted from a sample of the diabase sill, presumably at Hance Rapids, by Ford, Breed, and Mitchell,[27] while Elston and McKee obtained two K-Ar model ages of 913±40 Ma (for pyroxene in the diabase sill at Hance Rapids), and 954±30 Ma (for plagioclase from the diabase sill at Tapeats Creek). Additionally, Elston and McKee reported a total fusion $^{40}Ar/^{39}Ar$ age of 907±35 Ma for pyroxene from the diabase sill near Shinumo Creek and a $^{40}Ar/^{39}Ar$ isochron age of 904±100 Ma from seven-step incremental heating of a whole-rock sample from the diabase sill at Tapeats Creek.

Hendricks and Stevenson[28, 29] have summarized most of the details of the Unkar Group, including the diabase sills and dikes, and the Cardenas Basalt flows. Subsequently, while focusing on the Cardenas Basalt, Larson, Patterson, and Mutschler[30] found that, whereas the major-element chemistry of the diabase sills exhibited similarities and dissimilarities with the lower-member flows of the Cardenas Basalt,[31] the trace and rare earth element data from a sample of the sill at Hance Rapids show very similar variation patterns to those in the lower-member flows of the Cardenas Basalt. Only Ti and P contents were markedly higher in the sill, and the negative Eu anomaly for the sill was smaller than that for the lower-member Cardenas Basalt flows. Thus Larson, Patterson, and Mutschler suggested a common origin for the diabase of the sills and the basalt of the lower-member flows similar to continental flood basalts, except that the higher Ti and P contents of the diabase may indicate that the magma that fed the intrusions did not also directly feed the flows of the lower member. Alternately, they suggested that the higher silica, Ti and P contents of the basalt flows were due either to greater crustal contamination of the basalt magma on its passage to the earth's surface, or heterogeneity in the mantle source.

Finally, Austin and Snelling[32] obtained K-Ar data on five further samples, one from the diabase dike in Red Canyon adjacent to Hance Rapids, one from the diabase sill near Hance Rapids, and three from the sill near Bass Rapids (one diabase and two granophyre). The model ages ranged from 703±15 Ma to 895±20 Ma. When combined with the two samples analysed by Elston and McKee,[33] the K-Ar data yielded a K-Ar seven-point isochron age of 837±52 Ma, significantly discordant with the Rb-Sr five-point isochron age of 1070±30 Ma also obtained by Elston and McKee, and the Rb-Sr ten-point isochron age of 1103±66 Ma obtained by Larson, Patterson, and Mutschler[34] for the Cardenas Basalt flows and a sample of the Hance Rapids diabase sill. It was concluded that this discordance could not be explained by argon loss due to either resetting or leakage. Austin

and Snelling offered three alternative explanations—(a) argon inheritance, (b) argon mixing, or (c) change in the radioisotopic decay rates that affected ^{87}Rb and ^{40}K decay by different factors.

Sample Collection, Preparation and Analysis

Eleven whole rocks were collected from a composite section through the sill at Bass Rapids (north bank of the Colorado River at mile 107.6–108.0), the same section sampled by Hendricks and Lucchitta[35] some 800 meters east of Shinumo Creek. The samples were chosen to represent the overall petrographic variability within the complete thickness of the sill, as depicted in Fig. 2. These whole-rock samples were prepared by clean laboratory techniques as −200-mesh powders for chemical and isotopic analyses. Thin-sawed slices of the whole rocks were prepared as thin sections for petrographic analysis. One of the eight diabase samples representative of the sill was crushed to −140 to +270 mesh grains, and the various minerals within the powder were progressively concentrated by centrifugation in different heavy liquids, followed by further cleaning using a strong magnet. Six mineral phases were thus separated from whole-rock diabase sample DI-13 (biotite, clinopyroxene, normal plagioclase, high-density plagioclase, olivine, and magnetite). X-ray diffraction analysis and optical microscopy were used to confirm the identity and purity of the minerals concentrated.

XRAL Laboratories of Don Mills, Ontario, using XRF (x-ray fluorescence), ICP (inductively coupled plasma), and ICP-MS (mass spectrometer) methods, performed chemical analyses of the whole-rock powders for 67 elements. Whole rocks were subjected to standard K-Ar analysis by Geochron Laboratories, Cambridge, Massachusetts (R. Reesman, analyst) and Activation Laboratories, Ancaster, Canada (Y. Kapusta, analyst). Whole rocks and mineral separates were analyzed by mass spectrometry for Rb-Sr, Sm-Nd, and Pb-Pb isotopes by the University of Colorado (G.L. Farmer, analyst). The University of Colorado measurements of Sr, Nd, and Pb isotopes were carefully calibrated by internationally recognized standards. All the resultant isotopic data were then analyzed and isochrons plotted using the computer program called Isoplot.[36]

Petrography and Chemistry

The sill at Bass Rapids just east of Shinumo Creek is similar to other sills within the Unkar Group being composed of olivine diabase, but it is capped by granophyre (fig. 2), making this sill a classic example of in-place differentiation of a basaltic magma. The 6-m-thick granophyre consists predominantly of K feldspar (55–60%) and quartz (12–25%), with biotite, plagioclase, some clinopyroxene, and titanomagnetite making up the remaining 20–28%. The rock is holocrystalline, coarse-grained, and has a well-developed granophyric texture in which quartz, plagioclase, biotite, clinopyroxene, and titanomagnetite fill interstices between the orthoclase crystals. The transition between the granophyre and diabase below occurs over a vertical distance of less than 1 m and is a zone rich in biotite and accessory minerals.[37] Apatite makes up as much as 5–10% of the rock. ilmenite and sphene are prominent, and zircon with reaction halos occurs within the biotite grains.

The olivine diabase interior of the sill is medium- to coarse-grained, containing plagioclase (30–45%), olivine (20–35%), clinopyroxene (15–30%), titanomagnetite and ilmenite (5%), and biotite (1%), with accessory apatite and sphene. The texture is diabasic to subophitic, although a crude alignment of feldspar laths can be seen in many places. The plagioclase laths (composition $An_{45\text{-}60}$ [45–60% anorthite]) average 1.5 mm in length and are partially to completely altered to sericite. Both normal and reverse zoning of crystals are common. Anhedral to subhedral olivine crystals up to 1 mm in diameter are often partially altered along borders and fractures to chlorite, talc, magnetite, iddingsite, and serpentine. Fresh grain interiors have compositions of approximately Fo_{80} (80% forsterite) and interference colors that suggest normal zoning. Plagioclase laths and olivine grains are often enclosed by large, optically continuous, poikilitic clinopyroxene grains, giving the rock its subophitic texture. The clinopyroxene is brownish-pink, non-pleochroic augite which is usually fresh. Large irregular grains of titanomagnetite partly altered to hematite and biotite, as well as primary pleochroic brown biotite partially altered to chlorite, occupy interstices between the plagioclase and olivine grains.

The olivine concentration tends to increase towards the center of the sill, whereas the clinopyroxene decreases. Immediately below the granophyre the diabase contains about 5% modal olivine, which increases rapidly to 20–30% through the central part of the sill.[38] About 15 m above the base of the sill is an olivine-rich layer that contains about 50% modal olivine, and then the olivine content of the diabase decreases to about 10% near the base. Hendricks[39] and Hendricks and Lucchitta have suggested that this distribution of the olivine in the sill can be explained by the process of flow differentiation, which involves the movement of early-formed olivine grains away from the margins of the sill during flow of the intruding magma.[40–42] It is envisaged that, as the magma intrudes up through the conduit and then outward to form the sill, hydrodynamic forces concentrate toward the center of the moving mass the olivine crystals that have formed early in the cooling history of the magma, even before the emplacement of the sill. As the magma also moves laterally, gravity acting on the

Table 1. Whole-rock, major-element oxide and selected trace element analyses of 11 samples from the Bass Rapids sill, Grand Canyon, northern Arizona. Sample locations are shown in Fig. 1. (Analyst: XRAL Laboratories of SGS Canada, Don Mills, Ontario; January 1997 and February 2002).

Sample	DI-10	DI-11	DI-16	DI-17	DI-15	DI-18	DI-14	DI-13	DI-19	DI-7	DI-22
Position (from top)	2m	3.8m	5.5m	7.5m	21m	29m	49m	59m	71m	73m	86m
SiO2 (%)	60.4	60.9	57.8	46.5	45.4	46.0	45.2	44.7	44.5	45.2	46.2
TiO2 (%)	0.903	1.18	0.03	0.16	0.25	0.16	0.17	0.18	0.17	0.16	0.21
Al2O3 (%)	14.8	15.4	14.2	11.6	13.8	15.8	14.0	14.6	12.8	15.7	14.9
Fe2O3 (%)	5.96	4.79	8.24	16.2	14.1	12.5	13.3	12.4	12.6	10.3	13.5
MgO (%)	5.87	5.57	6.25	8.40	10.9	11.4	13.5	15.3	16.5	13.2	9.06
MnO (%)	<0.01	0.01	0.03	0.16	0.25	0.16	0.17	0.18	0.17	0.16	0.21
CaO (%)	0.27	0.09	0.65	4.16	6.89	8.13	7.68	7.80	4.16	8.48	7.15
Na2O (%)	0.57	1.47	1.63	3.15	2.06	2.18	1.86	1.87	1.71	1.93	2.23
K2O (%)	8.05	7.75	6.64	1.32	1.82	0.97	0.81	0.68	0.64	0.62	1.90
P2O5 (%)	0.03	0.02	0.32	1.23	0.51	0.26	0.28	0.09	0.27	0.19	0.43
S (%)	0.007	0.004	0.02	0.03	0.12	0.15	0.12	0.03	0.09	0.052	0.10
LoI (%)	2.85	2.90	2.95	3.15	2.2	1.75	1.85	1.2	2.7	2.4	2.45
TOTAL	99.8	100.2	100.0	99.0	99.9	100.4	100.3	100.1	100.4	99.4	100.30
Cr (ppm)	55	14	69	52	237	326	317	395	460	400	165
V (ppm)	108	116	72	200	195	142	140	88	131	110	231
Ni (ppm)	31	11	30	25	214	244	317	455	558	478	191
Co (ppm)	15	12	21	38	62	68	64	67	83	69	56
Cu (ppm)	3.4	7.9	15.6	51.4	98.3	129	63.9	30.3	55.0	31.0	101
Zn (ppm)	23.1	33.8	48.4	79.0	203	88.3	78.6	81.3	116	82.5	125
Rb (ppm)	104	106	87	23	39	23	18	16	23	14	51
Sr (ppm)	36	34	113	168	342	470	363	441	379	441	395
Zr (ppm)	228	313	349	342	160	92	116	82	116	68	161
Nb (ppm)	16	18	10	11	8	4	6	3	5	21	7
Ba (ppm)	567	633	613	327	322	184	134	167	161	239	352
Pb (ppm)	<2	<2	<2	7	7	<2	<2	<2	3	<2	5
Th (ppm)	9.4	12.0	12.2	6.4	<0.5	2.3	2.3	0.7	2.4	0.6	1.2
U (ppm)	1.9	2.5	4.0	4.8	1.7	<0.5	1.3	0.9	1.9	<0.5	0.9
La (ppm)	36.6	31.9	29.4	39.5	15.5	7.1	8.2	3.6	7.5	7.3	11.9
Ce (ppm)	80.8	68.9	65.5	94.0	38.2	17.8	20.5	8.2	18.8	16.9	29.7
Nd (ppm)	38.0	31.6	34.4	59.4	24.2	11.7	13.1	6.0	11.9	10.6	19.4
Sm (ppm)	8.1	6.2	7.9	13.3	6.3	3.1	3.3	1.5	2.9	3.2	4.6
Cl (ppm)	430	600	1050	580	1620	835	1070	363	842	954	2690

olivine crystals could have produced a gradational change in the olivine content from the lower contact upward, while causing an abrupt change in olivine from the upper contact downward. Once emplaced, crystallization of the remaining liquid magma within the sill would then have yielded the remaining minerals in relatively constant proportions.[43]

Although there is a general uniformity of the diabase throughout the sill, there are two types of textural variations, first described by Noble.[44] First, there are 'lumps' or 'balls' similar in mineralogy to the surrounding diabase, that is, olivine and plagioclase with augite filling interstices. The plagioclase laths in the lumps are up to 7.5 mm in length, filling embayments in large olivine crystals. The augite occurs as ophitic intergrowths with the plagioclase. Second, pegmatite veins consisting of plagioclase and augite with a very similar texture are found in the upper part of the sill. These textural variations undoubtedly represent segregation features produced during crystallization of the sill.

The lower chilled margin and contact of the sill with the underlying Hakatai Shale is covered, but is probably similar to the fine-grained chilled margins found in most of the other sills intruding the Unkar Group in Grand Canyon. The upper contact of the sill is marked by the 6-m thick capping of granophyre, the contact with

the overlying Hakatai Shale is sharp (fig. 2), and no xenoliths of Hakatai Shale are found in the granophyre, suggesting that it was not produced by assimilation of the shale. Instead, the transition zone between the granophyre and the diabase beneath it in the sill suggests that the granophyre was a residual magma that 'floated' to the top of the sill as the diabase crystallized, so that there was little late-stage mixing of it with the diabase part of the sill.[45]

Contact metamorphism of the Hakatai Shale has occurred above and below the sill, the shale being altered to a knotted hornfels (fig. 2). This contact metamorphism is greater below the sill than above it. The hornfels below the sill extends for 5m below the contact and forms a prominent outcrop. Biotite porphyroblasts as much as 0.25mm in size occur within 5cm of the contact with the sill, and at 10cm the shale is a knotted hornfels containing porphyroblasts of andalusite and cordierite(?) that have been replaced pseudomorphically by muscovite and green chlorite respectively. These porphyroblasts become larger and less numerous away from the sill, reflecting a slower rate and lower density of nucleation. No recrystallization of the shale has occurred beyond 5m below the sill contact, while the mineralogy of the metamorphism suggests that it was of low–medium grade.

The whole-rock, major element oxide and selected trace element analyses of the samples, whose locations are shown in Fig. 2, are listed in Table 1. The major element oxide percentages are very similar to those reported by Hendricks.[46] The granophyre as expected has a much higher SiO_2 content than the diabase making up the main portion of the sill, because the granophyre contains free quartz. Similarly, the diabase has a higher Fe_2O_3 and MgO content than the granophyre because of its olivine and augite content, the MgO concentration increasing towards the central part of the sill due to the higher olivine content there. Similarly, the higher Al_2O_3 and CaO values in the center of the sill would result from the concentration there of more calcic plagioclase. The high P_2O_5 content of sample DI-17 at the top of the diabase in close proximity to the granophyre is consistent with the apatite that is abundant in the transition zone. On a total alkalis-silica (TAS) diagram the diabase plots in the alkali olivine basalt field,[47, 48] using their own data and that of Hendricks and Lucchitta,[49] have suggested that chemically the diabase sills in the Unkar Group exhibit similarities and dissimilarities with the lower-member flows of the Cardenas Basalt, which are commonly regarded as the extrusive equivalents of these intrusive diabase sills.

Based on selected trace element data for one sample of the Hance Rapids sill, Larson, Patterson, and Mutschler[50] concluded that the variation in those data was very similar to trace element patterns for the lower-member flows of the Cardenas Basalt. The selected trace element data in Table 1 for the Bass Rapid diabase sill are also similar. Furthermore, the differences in trace element contents of the granophyre compared to the diabase are very obvious, and reflect the mineralogical differences. For example, Cr, Ni, Co, Cu, and Zn are much higher in the diabase than the granophyre, because of the olivine and trace sulfides found in the diabase that are not in the granophyre. In contrast, Ba, Rb, La, Ce, and Nd are much higher in the granophyre than in the diabase, reflecting differences in the feldspar contents of the two rock types, orthoclase being dominant in the granophyre, whereas plagioclase is dominant in the diabase and contains higher Sr. The higher content of Cl in the diabase parallels the higher content of P_2O_5 due to the presence of trace apatite. Zr is as expected higher in the granophyre where zircon is more likely to be in trace amounts.

Radioisotope Results

The K-Ar analytical data and K-Ar model 'ages' for all 11 samples are listed in Table 2. These model ages are calculated by the standard equation of Dalrymple and Lanphere[51] using the ratio of the abundances of $^{40}Ar^*$ (the radiogenic ^{40}Ar) to ^{40}K listed in Table 2. The model age method assumes no radiogenic ^{40}Ar was present when the basaltic magma cooled to form the diabase sill. The model 'ages' range from 656±15Ma (million years with one-sigma error) to 1053±24Ma, with the mean age being 816Ma (n=11). The wide variation in these model ages is not able to be explained readily, because they are not easily predicted by any possible sequence in the formation of the sill, such as the bottom and top of the sill cooling before the center of the sill, or the granophyre cooling before the diabase below. Indeed, there is no recognizable pattern, except that the model 'ages' are discordant from one another. The mean model 'age' for the granophyre is 863.3Ma (n=3), whereas the mean model 'age' for the diabase is 798.3Ma (n=8), but the model age for sample DI-14 in the center of the diabase sill is much older at 914±22Ma. Furthermore, pairs of samples very close to one another give highly discordant model ages, such as granophyre samples DI-10 and DI-11 which are only 1.8m apart and yet yield model ages of 895±20Ma and 721±14Ma, and diabase samples DI-19 and DI-7 which are only 2m apart and yet yield model ages of 866±24Ma and 728±20Ma respectively.

Fig. 3 is the ^{40}K versus ^{40}Ar diagram for the Bass Rapids diabase sill. The error bars plotted with the data are the estimated two-sigma uncertainties, and the strong linear trend that is apparent is plotted as an isochron

Table 2. K-Ar data for the Bass Rapids diabase sill, Grand Canyon, northern Arizona. (Analysis: Dr. R. Reesman, Geochron Laboratories, Cambridge, Massachusetts, and Dr. Y. Kapusta, Activation Laboratories, Ancaster, Canada).

Sample	Position (from top)	K_2O (wt%)	^{40}K (ppm)	$^{40}Ar^*$ (ppm)	$^{40}Ar^*$ (%)	Total ^{40}Ar (ppm)	$\frac{^{40}Ar}{^{36}Ar}$	^{36}Ar (ppm)	$\frac{^{40}K}{^{36}Ar}$	Model Age (Ma)	Uncertainty (Ma) (1 sigma)
DI-10	2 m	8.61	8.527	0.5737	96.4	0.5951	9155.4	0.000065	131184.6	895	±20
DI-11	3.8 m	8.245	8.166	0.4206	94.3	0.4460	5717.9	0.000078	104692.3	721	±14
DI-16	5.5 m	5.764	5.706	0.4281	92.85	0.4611	4875.0	0.000095	60063.2	974	±20
DI-17	7.5 m	1.413	1.399	0.1162	86.4	0.1345	2388.0	0.000056	24982.1	1053	±24
DI-15	21 m	2.661	2.634	0.1211	86.15	0.1406	2613.0	0.000054	48777.8	656	±15
DI-18	29 m	1.356	1.342	0.06572	76.45	0.08596	1370.0	0.000063	21301.6	692	±14
DI-14	49 m	0.959	0.950	0.06567	76.1	0.08629	1486.0	0.000058	16379.3	914	±22
DI-13	59 m	0.958	0.948	0.05014	83.45	0.06008	1896.0	0.000032	29625.0	737	±18
DI-19	71 m	0.778	0.770	0.04973	75.8	0.06561	1293.0	0.000051	15098.0	866	±24
DI-7	73 m	0.754	0.747	0.03893	80.0	0.04866	1623.3	0.000030	24900.0	728	±20
DI-22	86 m	2.157	2.135	0.11107	8.79	1.26359	3367.0	0.000375	5693.3	740	±22.4

using the Isoplot program of Ludwig[52] that utilizes the least-squares linear regression method of York.[53] All 11 samples were included in the regression calculation, although the assigned two-sigma errors were large. The isochron 'age' calculated from the slope of the line is 841.5±164 Ma (two-sigma error). The initial ^{40}Ar is zero, so this is consistent with the assumption of zero $^{40}Ar^*$ in the model age technique. This K-Ar isochron 'age' is discordant with the published five-point Rb-Sr whole-rock isochron 'age' for the sill of 1070±30 Ma.[54] Note also that the slope of the line is heavily influenced by the three granophyre data points with their high K contents due to their contained orthoclase. Because all the samples are cogenetic it was important that all are included in the calculation, even though it leads to a large two-sigma uncertainty in the isochron age. This large uncertainty must be due to more than analytical errors, and is thus indicative of the minor hydrothermal alteration present (plagioclase altered to sericite) and perhaps some contamination of the granophyre from the hornfels wall-rock during contact metamorphism.

Fig. 4 shows $^{40}K/^{36}Ar$ plotted against $^{40}Ar/^{36}Ar$ for the sill, based on the data in Table 2. The error bars again represent the two-sigma uncertainties in the data points, which again were large, with ten of the 11 samples included in the regression analysis. The calculated isochron age is therefore 844.7±179 Ma with an initial $^{40}Ar/^{36}Ar$ value of 249. This is much less than the present atmospheric $^{40}Ar/^{36}Ar$ value of 295.5, and suggests the possibility of a small Ar loss or that the regression line needs to be appropriately adjusted. This would reduce the isochron age, and make it even more discordant with the published Rb-Sr isochron age, even though it

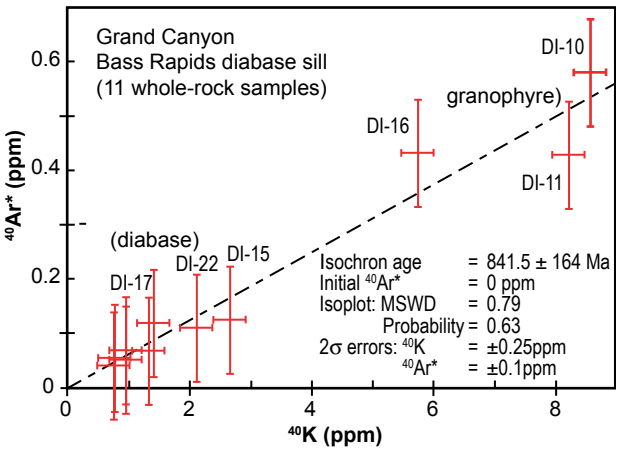

Fig. 3. ^{40}K versus ^{40}Ar in the Bass Rapids diabase sill, all 11 samples being used in the isochron and age calculations. The bars represent the two-sigma uncertainties.

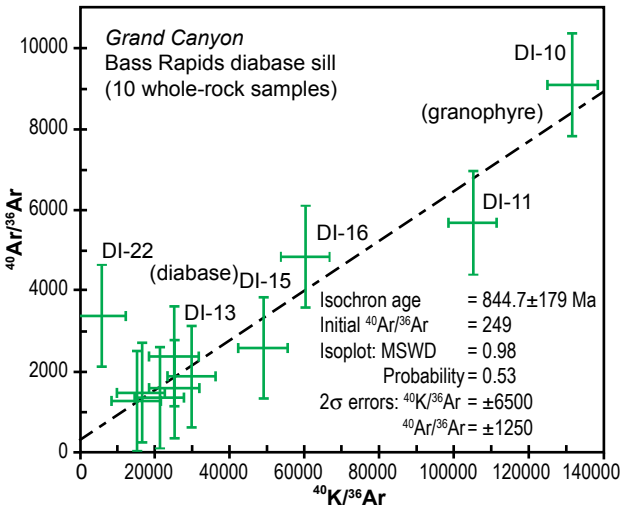

Fig. 4. $^{40}K/^{36}Ar$ versus $^{40}Ar/^{36}Ar$ in the Bass Rapids sill, all 11 samples being used in the isochron and age calculations. The bars show the two-sigma uncertainties.

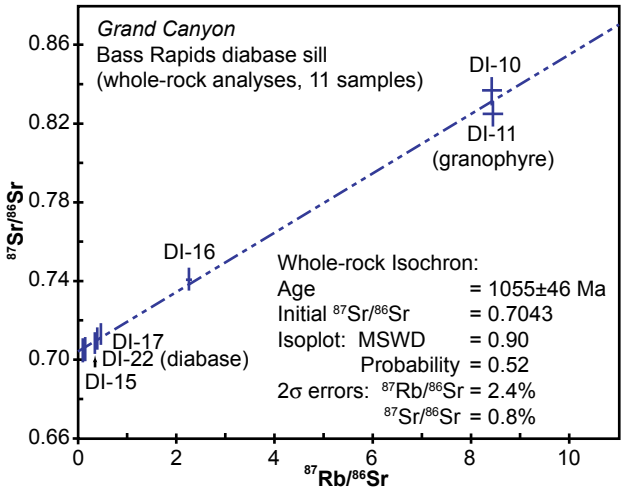

Fig. 5. $^{87}Sr/^{86}Sr$ versus $^{87}Sr/^{86}Sr$ diagram for the Bass Rapids diabase sill, all 11 whole-rock samples being used in the isochron and age calculations. The bars represent the two-sigma uncertainties.

would still be concordant with the K-Ar isochron age determined here and shown in Fig. 3. Alternately, the low $^{40}Ar/^{36}Ar$ value could indicate incorporation into the basaltic magma of 'primitive argon' thus inherited from its mantle source.[55]

The whole-rock Rb-Sr, Sm-Nd, and Pb-Pb radioisotopic data for all 11 samples from the sill are listed in Table 3. As anticipated, the radioisotopic ratios in the three granophyre samples are distinctly different to those obtained from the eight diabase samples. This reflects the major and trace element differences between these two rock types and their different mineralogies, the granophyre having a much higher K_2O content (table 2) than the diabase because of the abundant orthoclase in it. Thus, the Rb content of the granophyre is higher than that of the diabase, whereas the Sr content is higher in the diabase because it partitions with the Ca in plagioclase. The generally higher rare earth element and Pb contents of the granophyre likewise leads to significantly different radioisotopic ratios in the granophyre compared to the diabase. These differences are ideal for plotting of isochrons because of the larger spreads in the radioisotopic ratios.

Fig. 5 shows $^{87}Rb/^{86}Sr$ plotted against $^{87}Sr/^{86}Sr$ for the sill, based on the data in Table 3. The error bars again represent the two-sigma uncertainties in the data points, which were small. The regression analysis using the Isoplot program of Ludwig[56] yielded an excellent-fitting isochron with a high probability and low MSWD (mean square of weighted deviates—a measure of the ratio of the observed scatter of the data points from the best-fit line to the expected scatter from the assigned errors and error correlations). The resultant isochron age of 1055±46Ma is only marginally less than the five-point Rb-Sr isochron age of 1070±30Ma obtained by Elston and McKee.[57] At 0.7043, the initial $^{87}Sr/^{86}Sr$ for this isochron is virtually identical to the value of 0.70420±0.0007 obtained by Elston and McKee. Significantly, when we added the Rb-Sr data for the five Elston and McKee samples to that of our 11 samples the resulting regression analysis yielded an even better 16-point isochron with a higher probability (0.86) from the same two-sigma uncertainties for each of the data points. The isochron age of 1055±44Ma is identical, as is the initial $^{87}Sr/^{86}Sr$. Nevertheless, the uncertainty of ±44Ma is higher than the ±30Ma obtained by Elston and McKee, but a lot of this uncertainty is due to the poorer fit of the two high Rb granophyre samples DI-10 and DI-11.

Fig. 6 is the $^{147}Sm/^{144}Nd$ versus $^{143}Nd/^{144}Nd$ diagram for the Bass Rapids diabase sill using the data in Table 3. These whole-rock samples are tightly grouped showing that little variation within the Sm-Nd system exists within the whole rocks. No Sm-Nd age information can be derived from the 11 whole-rock samples. All eight diabase samples do suggest a line in Fig. 6, but Isoplot[58] attaches little age significance to it. The Sm-Nd mineral

Table 3. Whole-rock Rb-Sr, Sm-Nd, and Pb-Pb radioisotopic data for the Bass Rapids diabase sill, Grand Canyon, northern Arizona. (Analyst: Associate Professor G. L. Farmer, University of Colorado) at Boulder).

Sample	Position (from top)	Rb (ppm)	Sr (ppm)	$^{87}Rb/^{86}Sr$	$^{87}Sr/^{86}Sr$	Sm (ppm)	Nd (ppm)	$^{147}Sm/^{144}Nd$	$^{143}Nd/^{144}Nd$	$\varepsilon_{Nd}(t_o)$	T_{DM} (Ga)	$^{206}Pb/^{204}Pb$	$^{207}Pb/^{204}Pb$	$^{208}Pb/^{204}Pb$
DI-10	2m	101.5	35	8.4302	0.83703	8.25	37.8	0.132	0.512070	-11.08		22.948	15.933	42.233
DI-11	3.8m	95.8	33	8.439	0.82481	8.11	32.59	0.150	0.511992	-12.60		25.432	16.135	45.201
DI-16	5.5m	82.8	106	2.2643	0.741297	7.98	36.3	0.1329	0.512084	-10.81	1.80	21.923	15.878	41.482
DI-17	7.5m	24.2	154	0.4539	0.713329	14.55	62.4	0.1411	0.512391	-4.82	1.36	19.368	15.702	38.574
DI-15	21m	38.5	312	0.3568	0.709139	6.0	25.0	0.1456	0.512441	-3.84	1.34	17.255	15.475	36.981
DI-18	29m	21.8	422	0.1492	0.706359	3.08	12.5	0.1495	0.512458	-3.51	1.38	17.358	15.494	37.003
DI-14	49m	11.7	328	0.1026	0.705461	3.37	13.8	0.1473	0.512443	-3.80	1.37	18.355	15.561	38.154
DI-13	59m	15.4	383	0.1165	0.704818	2.65	10.8	0.1480	0.512438	-3.90	1.40	17.699	15.510	37.353
DI-19	71m	16.9	329	0.1487	0.705019	3.60	15.0	0.1452	0.512466	-3.36	1.28	17.260	15.452	36.854
DI-7	73m	11.5	347	0.0959	0.704502	1.64	6.04	0.164	0.512554	-1.64		17.407	15.480	37.005
DI-22	86m	51.3	371	0.4005	0.711306	5.13	21.1	0.1471	0.512446	-3.75	1.36	19.429	15.687	38.711

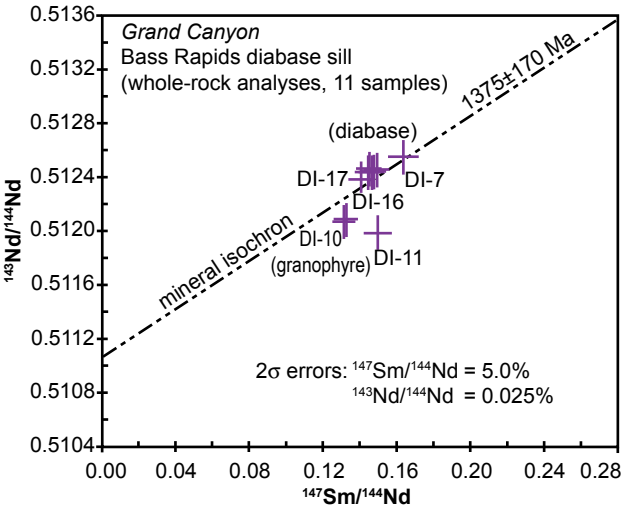

Fig. 6. $^{147}Sm/^{144}Nd$ versus $^{143}Nd/^{144}Nd$ diagram for all 11 whole-rock samples of the Bass Rapids diabase sill. The bars represent the two-sigma uncertainties. The Sm-Nd mineral isochron of Fig. 9 is shown for comparison. The eight diabase samples plot on the mineral isochron whereas the three granophyre samples (DI-10, DI-11, DI-16) do not, suggesting they have been contaminated from the hornfels wall-rock.

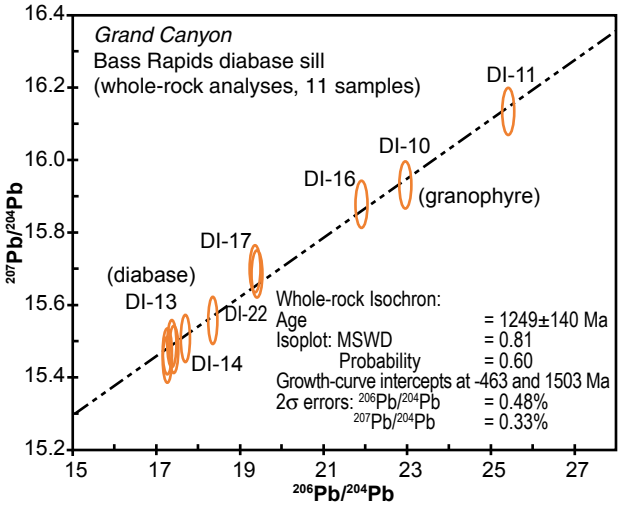

Fig. 7. $^{206}Pb/^{204}Pb$ versus $^{207}Pb/^{204}Pb$ diagram for the Bass Rapids diabase sill, using all 11 whole-rock samples in the isochron and age calculations. The error ellipses represent the two-sigma uncertainties

isochron (see below) is plotted in Fig. 6 and appears to pass through the eight whole-rock diabases. The three granophyre samples (DI-10, DI-11, and DI-16) plot on the diagram in a random scatter widely separated from any apparent relationship with the eight diabase samples, which is suggestive of contamination from the overlying hornfels wall-rock, perhaps by some assimilation of Nd.

Fig. 7 shows $^{206}Pb/^{204}Pb$ plotted against $^{207}Pb/^{204}Pb$ for the whole-rock samples from the Bass Rapids diabase sill. All 11 samples were used in the regression analysis and yielded an isochron fit with an 'age' of 1249±140 Ma, with a high probability and a low MSWD. The relatively large two-sigma uncertainty in the resultant age is largely due to the size of the two-sigma errors in the data points represented by the ellipses on the diagram. On the other hand, the three granophyre samples give a greater spread to the data which otherwise yields good regression statistics for the isochron.

Rb-Sr, Sm-Nd, and Pb-Pb radioisotopic data for the six minerals separated from the whole-rock diabase sample DI-13 are listed in Table 4. The strong partitioning of the relevant trace elements into the different mineral phases is evident as expected. For example, Rb is high in the biotite, whereas the Sr is high in the plagioclase. This was expected to provide a good spread in the radioisotopic data, and improve the statistics of the isochron fits.

Fig. 8 is the $^{87}Rb/^{86}Sr$ versus $^{87}Sr/^{86}Sr$ diagram for the six mineral fractions from sample DI-13, plus the whole rock. The regression analysis using the Isoplot program of Ludwig[59] produced an excellent isochron fit, with a very high probability and low MSWD. The resultant isochron age is 1059±48 Ma, the two-sigma uncertainty

Table 4. Mineral Rb-Sr, Sm-Nd, and Pb-Pb radioisotopic data for diabase samples DI-13 from the Bass Rapids sill, Grand Canyon, northern Arizona. (Analyst: Associate Professor G.L. Farmer, University of Colorado at Boulder.

Fraction	Rb (ppm)	Sr (ppm)	$^{87}Rb/^{86}Sr$	$^{87}Sr/^{86}Sr$	Sm (ppm)	Nd (ppm)	$^{147}Sm/^{144}Nd$	$^{143}Nd/^{144}Nd$	$\varepsilon_{Nd}(t_0)$	T_{DM} (Ga)	$^{206}Pb/^{204}Pb$	$^{207}Pb/^{204}Pb$	$^{208}Pb/^{204}Pb$
Whole-rock	15.4	383	0.1165	0.704818	2.65	10.8	0.1480	0.512438	-3.90	1.40	17.699	15.510	37.353
Biotite	92.2	187	1.4294	0.724746	2.37	11.3	0.1266	0.512225	-8.06	1.43	17.457	15.486	37.150
Clinopyroxene	0.74	32.8	0.0651	0.704166	5.19	14.3	0.2190	0.512922	+5.54		17.463	15.477	37.191
Plagioclase	28.5	784	0.1050	0.704769	0.63	9.4	0.0408	0.511448	-23.21	1.40	17.194	15.471	36.913
Olivine	0.36	7.62	0.1348	0.704752	1.15	5.9	0.1189	0.512097	-10.55	1.52	17.384	15.536	37.171
High-density Plagioclase	27.3	634	0.1244	0.704967	8.96	39.1	0.1385	0.512403	-4.58	1.29	17.085	15.461	36.791
Magnetite	1.01	7.98	0.3669	0.708408	0.88	27.1	0.0196	0.511161	-28.81	1.48	18.423	15.640	38.035

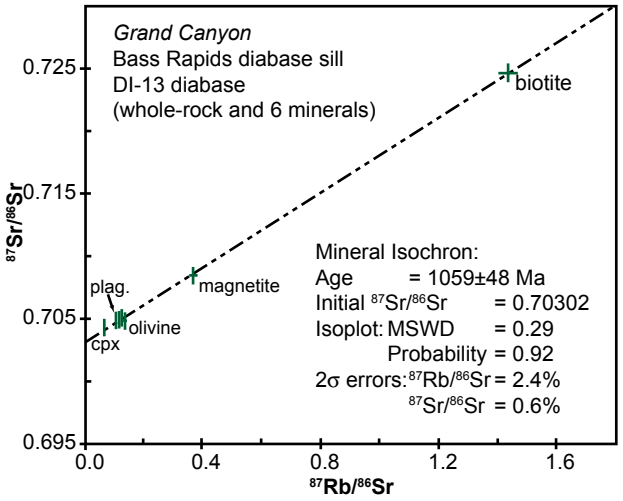

Fig. 8. $^{87}Rb/^{86}Sr$ versus $^{87}Sr/^{86}Sr$ diagram for six mineral fractions from diabase samples DI-13 (plus the whole-rock) from the Bass Rapids diabase sill. All seven data points were used in the isochron and age calculations, and the bars represent the two-sigma uncertainties.

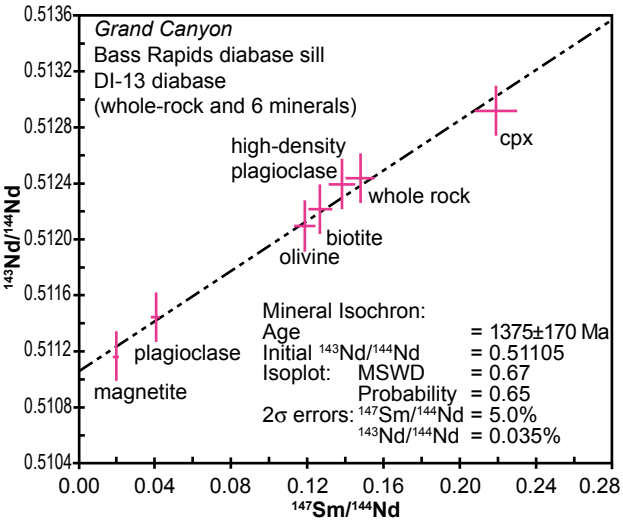

Fig. 9. $^{147}Sm/^{144}Nd$ versus $^{143}Nd/^{144}Nd$ diagram for six mineral fractions from diabase sample DI-13 (plus the whole-rock) from the Bass Rapids diabase sill. All seven points were used in the isochron and age calculations, and the bars represent the two-sigma uncertainties.

being moderate because the two-sigma error bars on the data points were also moderate. This mineral isochron age is, of course, totally concordant with the whole-rock Rb-Sr isochron age (1055±46Ma, Fig. 5), but at 0.70302 the initial $^{87}Sr/^{86}Sr$ is marginally lower than that for the whole-rock isochron.

Fig. 9 shows the $^{147}Sm/^{144}Nd$ versus $^{143}Nd/^{144}Nd$ diagram for the six mineral fractions, plus the whole rock, of sample DI-13 from the Bass Rapids diabase sill. The diagram shows an excellent large spread amongst the seven data points, from magnetite with the lowest $^{147}Sm/^{144}Nd$ ratio through to the highest $^{147}Sm/^{144}Nd$ ratio in the clinopyroxene. The regression analysis again produced an excellent isochron fit with a good probability and a low MSWD. The resultant mineral isochron age is 1375±170Ma. The relatively large two-sigma uncertainty in the isochron age is of course due to the relatively large two-sigma error bars for each of the data points, and to the scatter of some of the data points (for example, the whole rock and clinopyroxene) either side of the isochron (the line of best fit).

Finally, Fig. 10 shows $^{206}Pb/^{204}Pb$ plotted against $^{207}Pb/^{204}Pb$ for the six mineral fractions from sample DI-13, plus the whole rock, from the Bass Rapids diabase sill. These data are tightly grouped, showing that uranium is not strongly partitioned within the mineral phases within a single rock. Isoplot[60] shows no significant Pb-Pb age information can be derived from these seven data points. However, the Pb-Pb whole-rock isochron of Fig. 7 when plotted on Fig. 10 passes through the two-sigma error ellipses of all seven data points. Thus, the Pb-Pb mineral data appear to be concordant with the 1249±140Ma whole-rock Pb-Pb isochron.

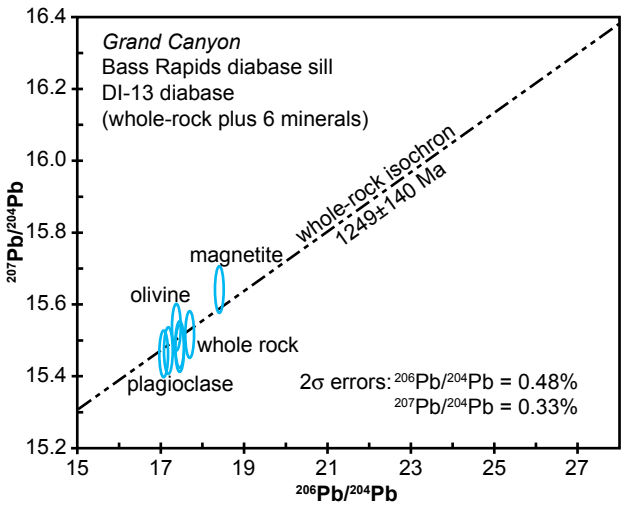

Fig. 10. $^{206}Pb/^{204}Pb$ versus $^{207}Pb/^{204}Pb$ diagram for six mineral fractions from diabase sample DI-13 (plus the whole-rock) from the Bass Rapids diabase sill. The error ellipses represent the two sigma uncertainties, and the Pb-Pb whole-rock isochron of Fig. 7 is shown for comparison.

Discussion

Isotope plots reveal extraordinary linearity within the ^{40}K-^{40}Ar, ^{87}Rb-^{87}Sr, ^{147}Sm-^{143}Nd, and ^{207}Pb-^{206}Pb-^{204}Pb radioisotope systems. Each of the four radioisotope pairs produces an eleven-point, whole-rock plot. The five data plots (Figs. 3 through 7) contain 55 data points with 51 points following linear trends. Remarkably, only four of the whole-rock data points plot significantly off the linear trends. Three of the data points plotting significantly off the line in Fig. 6 are easily explained by the granophyre's assimilation of neodymium due to

contamination from the adjoining hornfels just above the sill (Fig. 2). Certain hydrothermal conditions have been shown to cause rare earth element mobility in rhyolite and granite,[61] the Nd isotopes being perturbed during hydrothermal alteration. That such hydrothermal alteration of the granophyre in the sill has occurred during contact metamorphism with the overlying shale is evidenced by plagioclase altered to sericite and biotite altered to chlorite.

Some creationists may want to consider the possibility that the remarkably linear isotope ratios within the diabase and granophyre were derived, not by radioisotope decay, but by mixing of two different magmas. Such a model has been proposed by Giem[62] and discussed by Austin and Snelling.[63] We might suppose the sill at Bass Rapids was formed from a granophyre magma (higher K, Ar, Rb, Sm, Nd, and U) combined with different proportions of a diabase magma (lower K, Ar, Rb, Sm, Nd, and U). The mixing model supposes these two magmas, and their various magma mixtures, were never in an isotopically homogeneous condition. Isotopes from these two magma types may then have formed the mixing lines in Figs. 3 through 7 without radioisotope decay within the rocks. As pointed out by Austin,[64] mineral isochron plots provide the data critical for testing the magma mixing model. Mineral phases within any single rock should be homogeneous, because the mixing model supposes rocks crystallized from large, locally mixed, batches of melt, and since crystallization radioisotope decay has been minor. For the Bass Rapids diabase sill, however, radioisotopes differ significantly between mineral phases within diabase sample DI-13. Thus, significant radioisotope decay, not mixing, is the favored explanation of the extraordinary linearity. Furthermore, the petrographic and geochemical data from the Bass Rapids sill argues that 'unmixing' has occurred (chemical and gravitational segregation from an initially homogeneous, molten condition). The best explanation is exactly opposite the mixing model.

^{40}K-^{40}Ar, ^{87}Rb-^{87}Sr, ^{147}Sm-^{143}Nd, and ^{207}Pb-^{206}Pb-^{204}Pb radioisotope data provide strong evidence that the Bass Rapids diabase sill was intruded while in an isotopically mixed, homogeneous condition. Initially, the sill was chemically and isotopically homogeneous when the basaltic magma was intruded rapidly into the Hakatai Shale. The subsequent mineralogical segregation within the sill was produced by flow differentiation and gravitational settling, resulting in olivine diabase overlain by granophyre. At that time of intrusion the different parts of the newly formed sill had the same Ar, Sr, Nd, and Pb isotopic ratios. This must be, and is conventionally by definition, the agreed initial condition in order for radioisotopic dating of the diabase to be achievable.

What then can be said about the present isotopic ratios within whole rocks and minerals of the sill? Do parent-daughter radioisotope ratios produce a consistent picture of the 'age' of the sill? Two significant Rb-Sr whole-rock and mineral isochron plots (Figs. 5 and 8) appear to constrain the "age" of the diabase sill to 1055±46 Ma (two-sigma error). That is the currently accepted age of this Grand Canyon diabase according to Elston and McKee[65] and Larson, Patterson, and Mutschler[66] when the diabase sill was isotopically homogeneous with respect to Sr. However, the Sm-Nd mineral isochron plot (Fig. 9) is strongly linear giving the 'age' from initial homogeneous Nd as 1375±170 Ma (two-sigma error). Although the uncertainty associated with this Sm-Nd mineral isochron is larger, its 'age' is clearly discordant with Rb-Sr. How could the suite of minerals in sample DI-13 have Nd isotopes mixed at 1375±170 Ma (Fig. 9) but not have Nd remixed within the minerals by the event that thoroughly mixed the Sr isotopes within the minerals at 1059±48 Ma (Fig. 8)?

The Pb-Pb whole-rock isochron plot (Fig. 7) gives the 'age' from initial homogeneous Pb as 1249±140 Ma (two sigma-error), again discordant with Rb-Sr. How could the suite of whole rocks within the sill have Pb isotopes mixed at 1249±140 Ma (Fig. 7) but not have Pb remixed within the rocks by the event that thoroughly mixed the Sr isotopes at 1055±46 Ma (Fig. 5)? Both of these 'ages' are discordant with the K-Ar whole-rock isochron age (Fig. 3) of 841.5±164 Ma assuming no initial ^{40}Ar. Which of these is the true 'age' of the initial isotopic mixing? No internally consistent 'age' emerges from these data.

Indeed, Austin[67] has already documented that, when the mineral isochron method is applied as a test of the assumptions of radioisotopic dating, discordances inevitably result. According to Austin four categories of discordance are found in cogenetic suites of rocks—(a) two or more discordant whole-rock isochron ages, (b) a whole-rock isochron age older than the associated mineral isochron ages, (c) two or more discordant mineral isochrons from the same rock, and (d) a whole-rock isochron age younger than the associated mineral isochron ages. Our radioisotope data from the Bass Rapids diabase sill exhibit all four categories of isochron discordance. Thus the assumptions of radioisotopic dating must be questioned.

However, as already argued, there is corroborative evidence that the sill initially had a homogeneous mixture of the same Ar, Sr, Nd, and Pb isotopic ratios. Thus the assumption about the initial conditions for the sill and these radioisotope systems must be valid. Furthermore, the evidence for open-system behavior is limited to the neodymium in the Sm-Nd radioisotope system in the granophyre whole-rock samples (perturbed by contamination from the overlying hornfels wall-rock), so the closed-system assumption in this instance is not unreasonable. Therefore, could the differences in the calculated 'ages' above be caused by errors in determining

the 'constants' of radioisotope decay? According to Steiger and Jäger,[68] uranium decay constants are measured reproducibly to four significant figures. Therefore, no significant error occurs with Pb-Pb isochrons. Steiger and Jäger recommended the decay constant for ^{87}Rb of 1.42×10^{-11} that is in wide use, but Begemann et al.[69] recommend $1.406\pm0.008\times10^{-11}$. However, this small change would not close the discordance between the Rb-Sr and either the Pb-Pb or Sm-Nd systems. According to Begemann et al.,[70] researchers generally agree that the decay constant for ^{147}Sm has been determined to three significant figures (6.54×10^{-12}).

Our data indicate that the alpha emitters (^{238}U, ^{235}U, and ^{147}Sm) have yielded older ages than the beta emitters (^{87}Rb and ^{40}K) when used to date the same geologic event, that is, the intrusion of the Bass Rapids diabase sill. A logical explanation of these data is that the radioisotope decay of the various parent isotopes has not always proceeded at the rates described by modern decay 'constants,' the discordances being due to the different parent radioisotopes decaying at different rates over the same time period since the formation of the sill. In other words, the decay of these parent radioisotopes was accelerated by different amounts. Thus our data are consistent with the possibility that alpha decay was accelerated more than beta decay at some time or times in the past.

Furthermore, our data also show that there is a correlation between the present radioactive decay constants for these alpha and beta emitters and the 'ages' they have yielded for this same geologic event. Of the alpha emitters, ^{147}Sm has the smallest decay constant (and thus the longest half-life) and it yielded the oldest 'age,' a mineral isochron 'age' of 1375±170Ma (Fig. 9), compared to the Pb-Pb whole-rock isochron 'age' of 1249±140Ma (Fig. 7). Similarly, of the beta emitters, ^{87}Rb has the smaller decay constant (and thus the longer half-life) and it yielded the older 'ages,' a whole-rock isochron 'age' of 1055±46Ma (Fig. 5) and a mineral isochron 'age' of 1059±48Ma (Fig. 8), compared to the K-Ar whole-rock isochron 'age' of 841.5±164Ma (Fig. 3). Thus our data are also consistent with the possibility that the longer the half-life of the alpha or beta emitter the more its decay has been accelerated, relative to the other alpha or beta emitters, at some time or times in the past.

It is recommended that further similar studies of suitable rock units be undertaken to confirm these findings.

Conclusion

The distributions of radioisotopes and their daughter isotopes in the middle Proterozoic Bass Rapids diabase sill in Grand Canyon reveal a glaring problem with the assumptions of conventional radioisotopic dating. Even though several lines of evidence confirm that the daughter isotopes were homogeneously mixed when the basaltic magma was intruded initially to form the sill, the four analyzed radioisotope systems yield discordant whole-rock isochron 'ages' for this geologic event. Although significant discordance exists between the K-Ar, Rb-Sr, Sm-Nd, and Pb-Pb radioisotope methods, each method appears to yield concordant 'ages' internally between whole rocks and minerals. Internal concordance is best illustrated by the Rb-Sr whole-rock and mineral isochron 'ages' of 1055±46Ma and 1059±48Ma, respectively. Furthermore, the only evidence of open-system behavior is contamination of the whole-rock Sm-Nd radioisotope system in the granophyre immediately adjacent to the overlying hornfels wall-rock. Therefore, it is concluded that it is the constant decay rates assumption of conventional radioisotopic dating that is potentially invalid, and thus changing decay rates in the past could account for the demonstrated discordances between the resultant isochron 'ages.' Furthermore, our data are consistent with the possibilities that, at some time or times in the past, decay of the alpha emitters (^{238}U, ^{235}U, and ^{147}Sm) was accelerated more than decay of the beta emitters (^{87}Rb and ^{40}K), and the longer the present half-life of the alpha or beta emitter the more its decay was accelerated relative to the other alpha or beta emitters.

Acknowledgments

Grand Canyon National Park provided special use permits allowing access to the remote site and granting permission to collect rock samples. Private donors provided financial support through the RATE project, and the project preceding RATE, both administrated at the Institute for Creation Research.

References

1. Larson, E.E., P.E. Patterson, and F.E. Mutschler, 1994. Lithology, chemistry, age and origin of the Proterozoic Cardenas basalt, Grand Canyon, Arizona. *Precambrian Research* **65**:255–276.
2. McKee, E.H. and D.C. Noble, 1974. Rb-Sr age of the Cardenas lavas, Grand Canyon, Arizona. In, Karlstrom, T.N.V., G.A. Swann, and R.L. Eastwood (eds.), *Geology of northern Arizona*, pp.87–96. Flagstaff, Arizona: Rocky Mountain Sectional Meeting, Geological Society of America.
3. Elston, D.P. and E.H. McKee, 1982. Age and correlation of the late Proterozoic Grand Canyon disturbance, northern Arizona. *Geological Society of America Bulletin* **93**:681–699.
4. Austin. S.A. and A.A. Snelling, 1998. Discordant potassium-argon model and isochron 'ages' for Cardenas Basalt (Middle

Proterozoic) and associated diabase of Eastern Grand Canyon, Arizona. In, Walsh, R.E. (ed.), *Proceedings of the fourth international conference on creationism*, pp. 35–51. Pittsburgh, Pennsylvania: Creation Science Fellowship.
5. Elston and McKee, Ref. 3.
6. Hendricks, J.D. and G.M. Stevenson, 1990. Grand Canyon Supergroup: Unkar Group. In, Beus, S.S. and M. Morales (eds.), *Grand Canyon geology*, pp. 29–47. New York: Oxford University Press.
7. Hendricks, J.D. and G.M. Stevenson, 2003. Grand Canyon Supergroup: Unkar Group. In, Beus, S.S. and M. Morales (eds.), *Grand Canyon geology*, 2nd ed., pp. 39–52. New York: Oxford University Press.
8. Babcock, R.S., 1990. Precambrian crystalline core. In, Beus, S.S. and M. Morales (eds.), *Grand Canyon geology*, pp. 11–28. New York: Oxford University Press.
9. Ilg, B.R., K.E. Karlstrom, D.P. Hawkins, and M.L. Williams, 1996. Tectonic evolution of Paleoproterozoic rocks in the Grand Canyon: Insights into middle-crustal processes. *Geological Society of America Bulletin* **108**(9):1149–1166.
10. Karlstrom, K.E., B.R. Ilg, M.L. Williams, D.P. Hawkins, S.A. Bowring, and S.J. Seaman, 2003. Paleoproterozoic rocks of the granite gorges. In, Beus, S.S. and M. Morales (eds.), *Grand Canyon geology*, 2nd ed., pp. 9–38. New York: Oxford University Press.
11. Hendricks, J.D., 1972. *Younger Precambrian basaltic rocks of the Grand Canyon, Arizona*. Unpublished M.S. Thesis, Northern Arizona University, Flagstaff.
12. Hendricks, J.D., 1989. Petrology and chemistry of igneous rocks of middle Proterozoic Unkar Group, Grand Canyon Supergroup, Northern Arizona. In, Elston, D.P., G.H. Billingsley, and R.A. Young (eds.), *Geology of the Grand Canyon, Northern Arizona (with Colorado River guides)*, pp. 106–116. Washington, DC: American Geophysical Union.
13. Hendricks, J.D. and I. Lucchitta, 1974. Upper Precambrian igneous rocks of the Grand Canyon, Arizona. In, Karlstrom, T.N.V., J.A. Swann, and R.L. Eastwood (eds.), *Geology of northern Arizona*, pp. 65–86. Flagstaff, Arizona: Rocky Mountain Sectional Meeting, Geological Society of America.
14. Noble, L.F., 1910. Contributions to the geology of the Grand Canyon, Arizona: The geology of the Shinumo area. *American Journal of Science* **29**:369–386, 497–528.
15. Noble, L.F., 1914. The Shinumo quadrangle, Grand Canyon district, Arizona. *US Geological Survey Bulletin* **549**.
16. Maxson, J.H., 1967. *Preliminary geologic map of the Grand Canyon and vicinity, Arizona, eastern section*. Grand Canyon Natural History Association, scale 1:62500.
17. Maxson, J.H., 1968. *Preliminary geologic map of the Grand Canyon and vicinity, Arizona, western section*. Grand Canyon Natural History Association, scale 1:62500.
18. Hendricks, Ref. 11.
19. Hendricks, Ref. 12.
20. Hendricks and Lucchitta, Ref. 13.
21. Elston, D.P. and C.S. Grommé, 1974. Precambrian polar wandering from Unkar Group and Nankoweap Formation, eastern Grand Canyon. In, Karlstrom, T.N.V., J.A. Swann, and R.L. Eastwood (eds.), *Arizona, geology of northern Arizona*, pp. 97–117. Flagstaff, Arizona: Rocky Mountain Sectional Meeting, Geological Society of America.
22. Elston and McKee, Ref. 3.
23. Elston, D.P., 1989. Grand Canyon Supergroup, northern Arizona: Stratigraphic summary and preliminary paleomagnetic correlations with parts of other North American Proterozoic successions. In, Jenney, J.P. and S.J. Reynolds (eds.), *Geologic evolution of Arizona*, Digest 17, pp. 259–272. Tucson: Arizona Geological Society.
24. McKee and Noble, Ref. 2.
25. McKee, E.H. and D.C. Noble, 1976. Age of the Cardenas lavas, Grand Canyon, Arizona. *Geological Society of America Bulletin* **87**(8):1188–1190.
26. Elston and McKee, Ref. 3.
27. Ford, T.D., W.J. Breed, and J.S. Mitchell, 1972. Name and age of the upper Precambrian basalts in the eastern Grand Canyon. *Geological Society of American Bulletin* **83**(1):223–226.
28. Hendricks and Stevenson, Ref. 6.
29. Hendricks and Stevenson, Ref. 7.
30. Larson, Patterson, and Mutschler, Ref. 1.
31. Hendricks and Lucchitta, Ref. 13.
32. Austin, S.A. and A.A. Snelling, 1998. Discordant potassium-argon model and isochron 'ages' for Cardenas Basalt (middle Proterozoic) and associated diabase of eastern Grand Canyon, Arizona. In, Walsh, R.E., (ed.), *Proceedings of the fourth international conference on creationism*, pp. 35–51. Pittsburgh, Pennsylvania: Creation Science Fellowship.
33. Elston and McKee, Ref. 3.
34. Larson, Patterson, and Mutschler, Ref. 1.
35. Hendricks and Lucchitta, Ref. 13.
36. Ludwig, K.R., 2001. Isoplot/Ex (Version 2.49): The geochronological toolkit for Microsoft Excel. University of California Berkeley, Berkeley Geochronology Center, Special Publication No. 1a.
37. Hendricks, Ref. 12.
38. Hendricks and Lucchitta, Ref. 13.
39. Hendricks, Ref. 12.
40. Bhattacharji, S., 1967. Scale model experiments on flowage differentiation in sills. In, Wyllie, P.J. (ed.), *Ultramafic and related rocks*, pp. 69–70. New York: John Wiley and Sons.

41. Bhattacharji, S. and C.H. Smith, 1964. Flowage differentiation. *Science* **145**:150–153.
42. Simkin, T., 1967. Flow differentiation in the picritic sills of North Skye. In, Wyllie, P.J., (ed.), *Ultramafic and related rocks*, pp. 64–69. New York: John Wiley and Sons.
43. Simkin, Ref. 42.
44. Noble, Ref. 15.
45. Hendricks and Lucchitta, Ref. 20.
46. Hendricks, Ref. 37.
47. Hendricks, Ref. 37.
48. Larson, Patterson, and Mutschler, Ref. 1.
49. Hendricks and Lucchitta, Ref. 20.
50. Larson, Patterson, and Mutschler, Ref. 1.
51. Dalrymple, G.B. and M.A. Lanphere, 1969. *Potassium-argon dating: Principles, techniques and applications for geochronology.* San Francisco: W.H. Freeman.
52. Ludwig, Ref. 36.
53. York, D., 1969. Least squares fitting of a straight line with correlated errors. *Earth and Planetary Science Letters* **5**:320–324.
54. Elston and McKee, Ref. 3.
55. Dalrymple, G.B., 1969. $^{40}Ar/^{36}Ar$ analyses of historic lava flows. *Earth and Planetary Science Letters* **6**:47–55.
56. Ludwig, Ref. 36.
57. Elston and McKee, Ref. 3.
58. Ludwig, Ref. 36.
59. Ludwig, Ref. 36.
60. Ludwig, Ref. 36.
61. Poitrasson, F., C. Pin, and J.-L. Duthou, 1995. Hydrothermal remobilization of rare earth elements and its effects on Nd isotopes in rhyolite and granite. *Earth and Planetary Science Letters* **130**:1–11.
62. Giem, P.A.L., 1997. *Scientific theology*, pp. 144–146. Riverside, California: La Sierra University Press.
63. Austin and Snelling, Ref. 4.
64. Austin, S.A., 2000. Mineral isochron method applied as a test of the assumption of radioisotope dating. In, Vardiman, L., A.A. Snelling and E.F. Chaffin (eds.), *Radioisotopes and the age of the earth: A young-earth creationist research initiative*, pp. 95–121. El Cajon, California: Institute for Creation Research, El Cajon and St. Joseph, Missouri: Creation Research Society.
65. Elston and McKee, Ref. 3.
66. Larson, Patterson, and Mutschler, Ref. 1.
67. Austin, Ref. 64.
68. Steiger, R.H. and E. Jäger, 1977. Subcommission on geochronology: Convention on the use of decay constants in geo- and cosmochronology. *Earth and Planetary Science Letters* **36**:359–362.
69. Begemann, F., K.R. Ludwig, G.W. Lugmair, K. Min, L.E. Nyquist, P.J. Patchett, P.R. Renne, C.Y. Shih, I.M. Villa, and R.J. Walker, 2001. Call for improved set of decay constants for geochronological use. *Geochimica et Cosmochimica Acta* **65**:111–121.
70. Begemann, Ludwig, Lugmair, Min, Nyquist, Patchett, Renne, Shih, Villa and Walker, Ref. 69.